


# Efficient and selective oxidation of alcohols in water employing palladium supported nanomagnetic Fe<sub>3</sub>O<sub>4</sub>@hyperbranched polyethylenimine (Fe<sub>3</sub>O<sub>4</sub>@HPEI.Pd) as a new organic–inorganic hybrid nanocatalyst

Ali Ramazani<sup>1</sup>  | Mehdi Khoobi<sup>2,3</sup> | Fariba Sadri<sup>4</sup> | Roghayeh Tarasi<sup>1</sup> | Abbas Shafiee<sup>2</sup> | Hamideh Aghahosseini<sup>1</sup> | Sang Woo Joo<sup>5</sup>

<sup>1</sup> Department of Chemistry, University of Zanjan, P.O. Box 45195-313 Zanjan, Iran

<sup>2</sup> Department of Medicinal Chemistry, Faculty of Pharmacy and Pharmaceutical Sciences Research Center, Tehran University of Medical Sciences, Tehran 14176, Iran

<sup>3</sup> Medical Biomaterials Research Center, Tehran University of Medical Sciences, Tehran, Iran

<sup>4</sup> Department of Chemistry, Payame Noor University, P.O. Box 19395-3697 Tehran, Iran

<sup>5</sup> School of Mechanical Engineering, Yeungnam University, Gyeongsan 712-749, Republic of Korea

## Correspondence

Ali Ramazani, Department of Chemistry, University of Zanjan, PO Box 45195-313, Zanjan, Iran.  
Email: aliramazani@gmail.com

## Funding information

National Research Foundation of Korea, Grant/Award Number: NRF-2015-002423

Palladium immobilized magnetic nanoFe<sub>3</sub>O<sub>4</sub>@hyperbranched polyethylenimine (Fe<sub>3</sub>O<sub>4</sub>@HPEI.Pd) was prepared according to a simple and cost effective pathway and it was employed as a new efficient and selective organic–inorganic hybrid nanocatalyst for the aqueous oxidation of primary and secondary alcohols to their corresponding products in good yields applying oxone (potassium hydrogen monopersulfate) and H<sub>2</sub>O<sub>2</sub> as an oxidant at room temperature. Moreover, the catalytic system was reused at least 13 times without significant loss of activity. The complete characterization of this efficient nanocatalyst was investigated by FTIR, UV–Vis, TEM, SEM, XRD, TGA, VSM, ICP and EDX techniques.

## KEYWORDS

alcohols, carbonyl compounds, nanomagnetic catalyst, oxidation, oxone

## 1 | INTRODUCTION

One of the significant transformations in organic chemistry is the oxidation of alcohols. A wide variety of metal and non-metal-based stoichiometric reagents has been developed in order to oxidize primary and secondary alcohols to the corresponding aldehydes, ketones and carboxylic acids.<sup>[1–4]</sup> Catalytic oxidation of non-activated aliphatic alcohols with molecular oxygen is rather challenging, especially in an aqueous medium in the absence of an additional base.<sup>[5]</sup> Although these processes are more environmentally friendly, they often

need expensive metals and/or other reagents. Traditional methods utilizing stoichiometric quantities of inorganic oxidants such as chromium (VI) reagents, permanganates, or *N*-chlorosuccinimide (NCS) are not environmentally benign. Even grave recent developments of hypervalent iodine reagents, which are popular in organic synthesis, also cause severe environmental problems. Thus, the development of greener oxidation systems continues using less poisonous catalysts, oxidants, and solvents became a crucial aim for the catalysis and the search for environmentally friendly as well as economical oxidation processes.<sup>[6–9]</sup> The oxone is

relatively stable compound at room temperature, readily available, and a convenient and therefore is utilized for various transformations in organic synthesis.<sup>[10–19]</sup> Selective oxidation processes represent a large class of organic reactions, which the improvement of green catalysts is a major concern in the field of chemical reactions. Some defects have been found regarding homogeneous catalysts. For example, difficult workup of the perilous metal residues, and lack of recycling methods, which make them inconvenient for large-scale applications.<sup>[20]</sup>

The use of palladium catalysts for the oxidation of alcohols to aldehydes and ketones in the presence of various types of oxidants is well known. Recently, the advantages of using molecular oxygen as the oxidant in the Pd-catalyzed oxidation of alcohols have been explored. The magnetic Pd catalyst showed high activity in the oxidation of HMF to FDCA in water.<sup>[21–23]</sup> In heterogeneous reaction, tedious methods like centrifugation and filtration are utilized to recover catalysts and end in loss of solid catalyst in the separation process. The magnetic nanoparticles in a variety of solid matrices allows the combination of well-known procedures for catalyst heterogenization and magnetic separation that supplies a convenient method to remove and recycle magnetized species by utilizing an appropriate magnetic field.<sup>[24,25]</sup>

Iron oxide magnetic nanoparticles have attracted growing interest owing to their unique properties and potential applications in various fields, such as magnetically assisted drug delivery, magnetic resonance imaging (MRI) contrast agents, hyperthermia, and magnetic separation of biomolecules.<sup>[26–28]</sup> Most of these utilizations require the nanoparticles to be chemically stable, uniform in size, and well scattered in liquid media. As a result of anisotropic dipolar attraction, pristine nanoparticles of iron oxides tend to aggregate into large groups and thus lose the particular qualities associated with single-domain, magnetic nanostructures. Surfactants with relatively high concentrations are often required to prevent such an aggregation. The presence of large amounts of surfactants in these systems may severely affect its utilizations. It has been illustrated that the formation of a passive coating of inert materials such as polymers, carbons, and silicas on the surfaces of iron oxide nanoparticles could help prevent their aggregation in liquid and make their chemical stability better and better.<sup>[29–34]</sup>

In this work, the amine groups of hyperbranched polyethylenimine (HPEI) were reacted with the epoxy groups of [3-(2,3-Epoxypropoxy)propyl]trimethoxysilane (EPO) and then the resulted polymer was grafted to the Fe<sub>3</sub>O<sub>4</sub> magnetic nanoparticles (MNPs) *via* the reaction of its trimethoxysilane group with OH groups of MNPs. Finally, it is assumed that the prepared Fe<sub>3</sub>O<sub>4</sub>@HPEI has good nitrogenous ligand for palladium (or cobalt and copper) chelating and could be

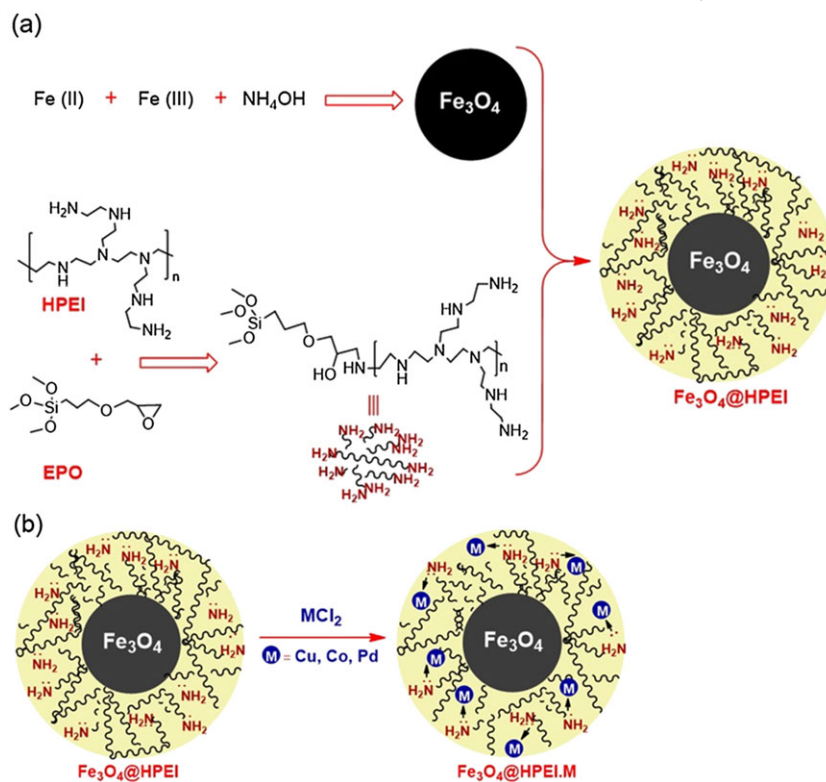
effective for uniform reoxidation of Pd(0) in the cycle of reaction<sup>[35]</sup> (Scheme 1). The prepared nanomagnet (Fe<sub>3</sub>O<sub>4</sub>@HPEI.Pd) was employed as a high active and reusable catalyst through magnetic separation for the selective oxidation of alcohols with oxone in the presence of water at room temperature.

## 2 | EXPERIMENTAL

### 2.1 | Materials and methods

[3-(2,3-Epoxypropoxy)propyl]trimethoxysilane (EPO, 98% purity), ferric chloride hexahydrate (FeCl<sub>3</sub>·6H<sub>2</sub>O), ferrous chloride tetrahydrate (FeCl<sub>2</sub>·4H<sub>2</sub>O), palladium chloride and alcohols were purchased from Merck (Darmstadt, Germany). Hyperbranched polyethylenimine (HPEI, Mw = 60,000) was purchased from Sigma-Aldrich.

The IR spectra were taken using Nicolet FT-IR Magna 550 spectrographs (KBr disks). The UV–Vis spectrum of catalyst (dispersed in ethanol) was recorded at room temperature on a UV–visible spectrophotometer (model: dr5000). The thermogravimetric analyses were performed using a TGA Q50 thermogravimetric analyzer of a TGA instrument with a heating ramp of 10 °C min<sup>−1</sup> under argon flow from room temperature to 800 °C. The structural properties of synthesized nanoparticles were analyzed by X-ray powder diffraction (XRD) with a XPert MPD advanced diffractometer using Cu (Kα) radiation (wavelength: 1.5406 Å) at room temperature in the range of 2θ from 4 to 120° with a scanning rate of 0.02° S<sup>−1</sup>. The magnetic properties of samples were detected at room temperature using vibrating sample magnetometer (VSM, Meghnatis Kavir Kashan Co., Kashan, Iran). The particle size and morphology of the surfaces of the samples were analyzed by a scanning electron microscopy (VEGAII TESCAN) with an acceleration voltage of 15 kV. The disc was pasted with copper tape, and the sample was dispersed over the tape. The disc was coated with gold in an ionization chamber. An EM208 Philips Company transmission electron microscopy (TEM) was used. Samples were prepared by placing a droplet 1 (μl) of nanocomposite dispersion latex, along with a droplet of water, on a copper grid covered by Formvar foil (200 mesh), dried and analyzed. The concentration of Pd in the Fe<sub>3</sub>O<sub>4</sub>@HPEI.Pd was analyzed by inductively coupled plasma emission spectroscopy (ICP) using an ICP-OES (Model: VISTA-PRO) instrument. Energy dispersive X-ray analysis (EDX) was carried out on Rontec (Germany) electron microscope. The parameters were as follows: accelerating voltage 15 kV. <sup>1</sup>H–NMR spectra were recorded on a Bruker Ultra shield-300 MHz spectrometer. The aliphatic products detected by GC-FID (VARIAN C-P-3800 with FID detector, column CP-Sil 5 CB30m × 0.32 mm).



**SCHEME 1** (a) preparation of magnetic nano  $\text{Fe}_3\text{O}_4@\text{HPEI}$ ; (b) palladium, cobalt and copper chelation with the nitrogenous ligands in  $\text{Fe}_3\text{O}_4@\text{HPEI}$  to prepare  $\text{Fe}_3\text{O}_4@\text{HPEI.M}$  (b)

## 2.2 | Preparation of catalyst

### 2.2.1 | Preparation of $\text{Fe}_3\text{O}_4$ MNPs

Iron oxide nanoparticles were synthesized by the co-precipitation of  $\text{Fe}^{2+}$  and  $\text{Fe}^{3+}$  ions (molar ratio 1:2) in ammonia solution.<sup>[36]</sup> Briefly,  $\text{FeCl}_2 \cdot 4\text{H}_2\text{O}$  (1.6 g) and  $\text{FeCl}_3 \cdot 6\text{H}_2\text{O}$  (4.32 g) were dissolved in deionized water (20 ml) under a nitrogen atmosphere and vigorous stirring with mechanical stirrer. Then,  $\text{NH}_3 \cdot \text{H}_2\text{O}$  (28 wt.%, 25 ml) was added dropwise to the solution under vigorous stirring and the solution was heated to 70 °C. The reaction proceeded for 2 h at 70 °C, and then the temperature was increased to 85 °C to vapor the residual ammonia. The resulting black dispersion was magnetically separated by an external magnet and washed repeatedly with deionized water.

### 2.2.2 | Covalently grafting of HPEI to $\text{Fe}_3\text{O}_4$ MNPs (preparation of $\text{Fe}_3\text{O}_4@\text{HPEI}$ )

To a stirred solution of 150 ml dry toluene containing 3 mmol of HPEI, 1 mmol of EPO was added. The resulting mixture was allowed to react at 80 °C for 24 h. To this solution, 2.5 g of dispersed  $\text{Fe}_3\text{O}_4$  MNPs in 25 ml of ethanol were added and the solution was then stirred at 80 °C for 24 h.  $\text{Fe}_3\text{O}_4@\text{HPEI}$  was magnetically isolated by an external magnet and washed repeatedly with methanol and ethanol. Then, it was Soxhleted with ethanol during 24 h to remove the

unreacted substrates and by products. It was magnetically separated by an external magnet again and dried at 40 °C for several days.<sup>[37]</sup>

### 2.3 | Preparation of nanomagnetic hyperbranched polyethylenimine-supported palladium catalyst ( $\text{Fe}_3\text{O}_4@\text{HPEI.Pd}$ )

$\text{Fe}_3\text{O}_4@\text{HPEI}$  (0.3 g) was charged into a round-bottomed flask containing an acetonitrile solution (10 ml) and sonicated for 20 minutes. Palladium chloride (0.6 mmol) was charged into another round-bottomed and sonicated for 20 minutes. Then, this mixture was added drop wise to the above mixture under an argon atmosphere and sonicated for 30 minutes. Then, this mixture stirred under an argon atmosphere for 48 h. The resultant catalyst was filtered off and washed with acetonitrile followed by acetone. The residue was dried in a vacuum oven for 24 h.<sup>[35]</sup> In addition, the same procedure was used Co and Cu incorporation into the nanomagnetic catalyst by using cobalt and copper chloride.

### 2.4 | General procedure for the oxidation of alcohols

Alcohol (1 mmol), water (2 ml) and catalyst (1 mol% of Pd, 30 mg) were added into a round-bottomed flask. The reaction

mixture was stirred for two minutes, and then oxone (0.6 mmol) was added in three portions during 15 minutes. The reaction mixture was stirred at room temperature. Progress of the reaction was followed by TLC (EtOAc-cyclohexane, 2:10) in comparison with the standard samples of corresponding alcohols and carbonyl compounds. After the completion of the reaction, the product was extracted with dichloromethane. The organic phase was evaporated under reduced pressure to give the corresponding aromatic products. Purification of the residue using flash column chromatography (silica gel) provided the pure carbonyl compounds. The products were characterized *via* comparison their spectral data (IR,  $^1\text{H}$  NMR) with authentic samples. The aliphatic products in dichloromethane were dried by using anhydrous  $\text{MgSO}_4$  and detected by GC-FID in comparison with the standard samples of corresponding alcohols and carbonyl compounds. The GC yields of the aliphatic products were calculated based on their corresponding gas chromatogram. The selectivity of the oxidized products was determined from their  $^1\text{H}$  NMR spectra of corresponding crude samples.

### 3 | RESULTS AND DISCUSSION

#### 3.1 | Characterization of the catalyst

Figure 1 shows the FT-IR spectra of  $\text{Fe}_3\text{O}_4$  MNPs and  $\text{Fe}_3\text{O}_4@\text{HPEI}$ . HPEI grafted on the  $\text{Fe}_3\text{O}_4$  by coupling agent EPO can be seen clearly from the occurrence of the strongly absorbing region of  $1110\text{--}1000\text{ cm}^{-1}$  results from the vibration of Si-O-H and Si-O-Si groups,  $584\text{ cm}^{-1}$  corresponds to the Fe-O bond and the bands at around  $2924\text{ cm}^{-1}$  and  $2831\text{ cm}^{-1}$  which are attributed to the aliphatic C-H bands. These values are in accord with the previously reported data.<sup>[38]</sup> The produced band  $1581\text{ cm}^{-1}$  are ascribed to the stretching vibration of the C-N bonds. The appearances of these bands reveal covalently link of HPEI

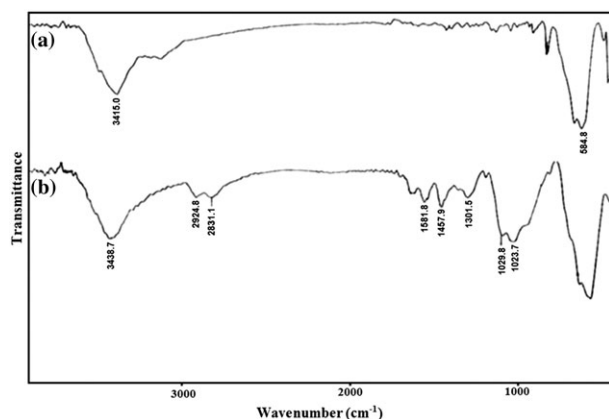


**FIGURE 1** FT-IR spectra of the  $\text{Fe}_3\text{O}_4$  (a) and  $\text{Fe}_3\text{O}_4@\text{HPEI}$  (b)

on the surfaces of  $\text{Fe}_3\text{O}_4$  (Figure 1b). Comparing the IR peaks of  $\text{Fe}_3\text{O}_4@\text{HPEI}$  with the FT-IR spectra of metal (Pd, Cu or Co) coated nanocatalysts (Supplementary data, Figure S1), the similar bands suggest the presence of  $\text{Fe}_3\text{O}_4@\text{HPEI}$  in the structure of metal (Pd, Cu or Co) coated nanocatalysts.

The crystalline structures of the obtained  $\text{Fe}_3\text{O}_4$ ,  $\text{Fe}_3\text{O}_4@\text{HPEI}$  and  $\text{Fe}_3\text{O}_4@\text{HPEI.Pd}$  were determined by XRD analysis (Figure 2). The position and relative intensity of all diffraction peaks matched well with standard  $\text{Fe}_3\text{O}_4$ .<sup>[39]</sup> The results indicate that the shape of the MNPs is inverse spinel  $\text{Fe}_3\text{O}_4$  with a face-centered cubic (fcc) structure, suggesting the sample has a cubic crystal system. From comparing the diffraction patterns of  $\text{Fe}_3\text{O}_4$  with  $\text{Fe}_3\text{O}_4@\text{HPEI}$  and  $\text{Fe}_3\text{O}_4@\text{HPEI.Pd}$ , the broadening of diffraction peaks indicated that the prepared  $\text{Fe}_3\text{O}_4$  is in polycrystalline form. All the diffraction peaks could be readily indexed to (1 1 1), (2 2 0), (2 0 0) lattice planes of a face-centered cubic (fcc) Pd crystal structure and (2 2 0), (3 1 1), (2 2 2), (4 0 0), (5 1 1), (4 4 0) lattice planes of fcc  $\text{Fe}_3\text{O}_4$ .<sup>[40]</sup>

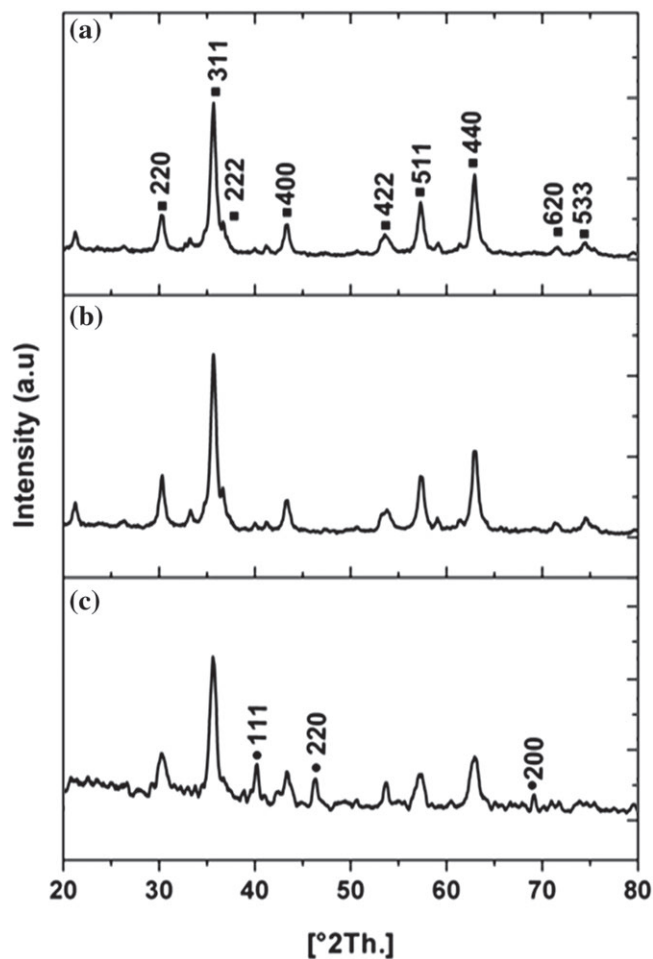


**FIGURE 2** XRD patterns of the  $\text{Fe}_3\text{O}_4$  (a),  $\text{Fe}_3\text{O}_4@\text{HPEI}$  (b) and  $\text{Fe}_3\text{O}_4@\text{HPEI.Pd}$  (c)



In the UV–Vis absorption spectra of  $\text{Fe}_3\text{O}_4@\text{HPEI}$  and  $\text{Fe}_3\text{O}_4@\text{HPEI}.\text{Pd}$  (Supplementary data, Figure S2), position and relative intensity of absorptions are matched well with previously reported.<sup>[41,42]</sup> The absorption peaks observed for  $\text{Fe}_3\text{O}_4@\text{HPEI}$  at  $\lambda_{\text{max}} = 210$  nm. The UV–vis spectrum of  $\text{Fe}_3\text{O}_4@\text{HPEI}.\text{Pd}$ , displayed the characteristic absorption band with decreasing absorptivity at 225 nm in the presence of  $\text{Pd}^{2+}$ .

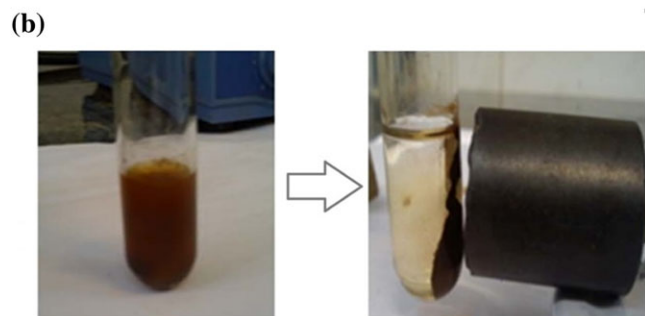
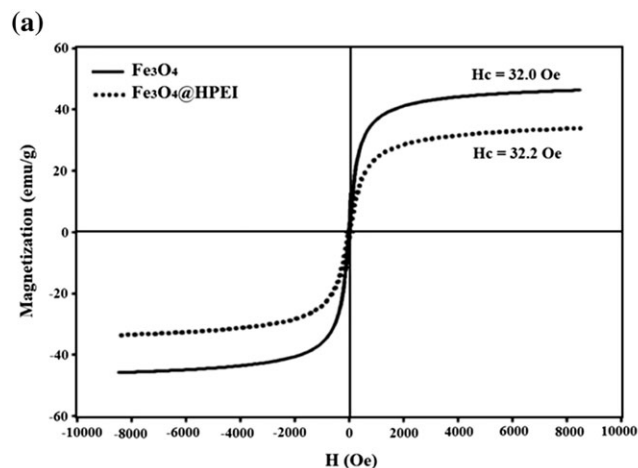


**FIGURE 3** (a) magnetic behavior of  $\text{Fe}_3\text{O}_4$  and  $\text{Fe}_3\text{O}_4@\text{HPEI}$ ; (b)  $\text{Fe}_3\text{O}_4@\text{HPEI}.\text{Pd}$  catalyst removing by an external magnet in an alcohol oxidation reaction

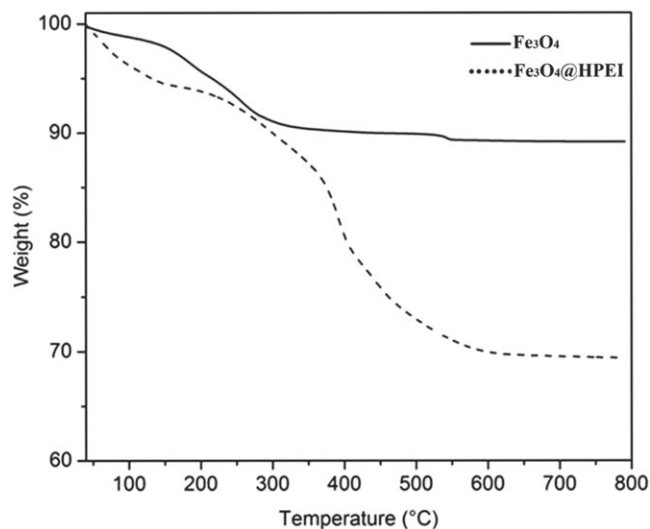


**FIGURE 4** TGA analyses of  $\text{Fe}_3\text{O}_4$  and  $\text{Fe}_3\text{O}_4@\text{HPEI}$

Magnetic behavior of the obtained  $\text{Fe}_3\text{O}_4$  MNPs and  $\text{Fe}_3\text{O}_4@\text{HPEI}$  is shown in Figure 3a. The superparamagnetic behavior was reflected in the low residual magnetization ( $M_r$ )

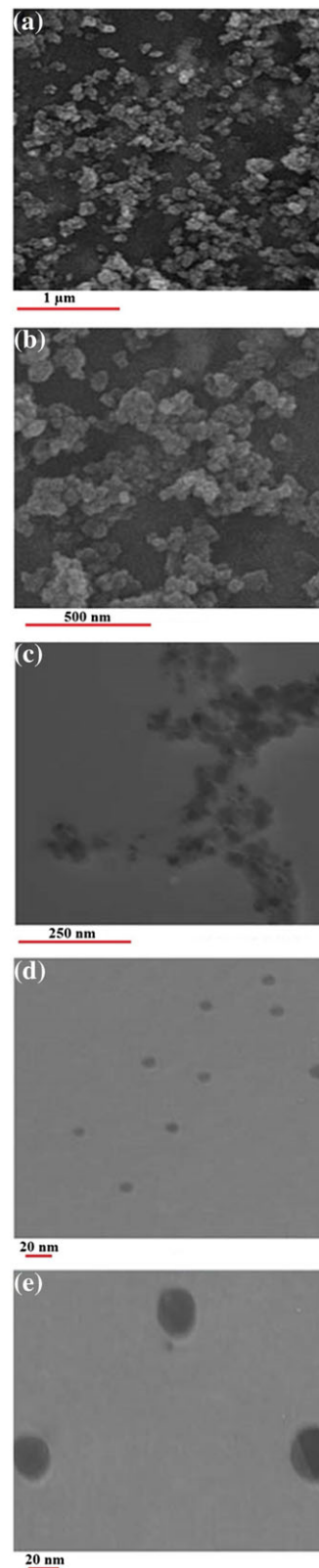


**FIGURE 5** SEM images of  $\text{Fe}_3\text{O}_4$  (a) and  $\text{Fe}_3\text{O}_4@\text{HPEI}$  (b) and TEM images of  $\text{Fe}_3\text{O}_4$  (c) and  $\text{Fe}_3\text{O}_4@\text{HPEI}$  (d,e)

and coercivity ( $H_c$ ) values.<sup>[43]</sup> The coercive field ( $H_c$ ), which represents the required force to rotate the magnetization vector of a magnet out of its equilibrium direction, and specific saturation magnetization ( $\sigma_s$ ) values for the prepared MNPs were calculated as 32 Oe and 46.4 emu g<sup>-1</sup> whereas for Fe<sub>3</sub>O<sub>4</sub>@HPEI were calculated as 30.2 Oe and 33.8 emu g<sup>-1</sup>. The saturation magnetization of Fe<sub>3</sub>O<sub>4</sub>@HPEI was less than that of Fe<sub>3</sub>O<sub>4</sub>, which might be attributed to the silica and polymer coating on the surface of the Fe<sub>3</sub>O<sub>4</sub>. Figure 3b shows Fe<sub>3</sub>O<sub>4</sub>@HPEI.Pd as a catalyst was easily separated from the products by exposure of the reaction vessel to an external magnet and decantation of the reaction mixture.

The amount of EPO and HPEI groups on the MNPs was measured by TGA analyses (Figure 4). The weight loss in the first step (25–150 °C) was attributed to the vaporization of water (about 10%). The second weight loss observed at temperatures higher than 200 °C was corresponded to the slow decomposition of the higher molecular weight species that present in the magnetic nanospheres. According to the TGA results, the percentage of grafting density of the HPEI has been found to be about 20%.

Figure 5 shows the SEM and TEM images of Fe<sub>3</sub>O<sub>4</sub> and Fe<sub>3</sub>O<sub>4</sub>@HPEI. The TEM analysis suggests that the MNPs are almost spherical (Figure 5c-e). These results are in good

harmony with the XRD analyses (Figure 2). The results show that the diameter of pristine Fe<sub>3</sub>O<sub>4</sub> nanoparticles is about 20–30 nm. After the grafting of HPEI on the magnetic nanospheres, the morphology of the resulting Fe<sub>3</sub>O<sub>4</sub>@HPEI was shown to resemble their original state.

The ICP analyzing shows that 3.44% of Fe<sub>3</sub>O<sub>4</sub>@HPEI.Pd weight is palladium, Fe<sub>3</sub>O<sub>4</sub>@HPEI.Cu has 8.87% copper and Fe<sub>3</sub>O<sub>4</sub>@HPEI.Co has 8.19% cobalt. The elemental composition of the Fe<sub>3</sub>O<sub>4</sub>@HPEI.Pd was also analyzed by the energy-dispersive X-ray (EDX) spectrum and the presence of palladium inside the catalyst was further confirmed (Supplementary data, Figure S3). From the EDX spectrum, it can be seen obviously the presence of Pd peaks, which confirm the presence of Pd.

The electronic properties and surface chemical compositions of Fe<sub>3</sub>O<sub>4</sub>@HPEI were investigated by XPS technique (Supplementary data, Figure S4). The characteristic peaks at 159 eV, 285 eV, 405 eV, and 536 eV corresponded to S2p, C 1 s1/2, N 1 s1/2 and O1s1/2, respectively.<sup>[44]</sup>

### 3.2 | Optimization of alcohol oxidation conditions

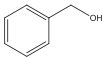
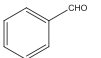
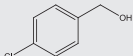
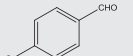
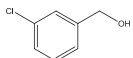
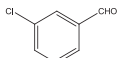
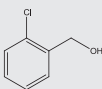
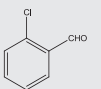
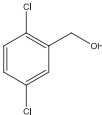
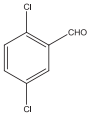
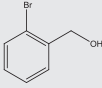
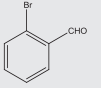
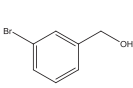
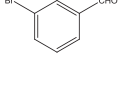
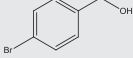
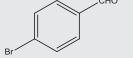
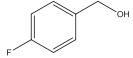
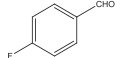
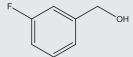
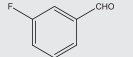
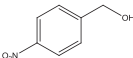
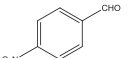
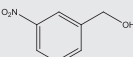
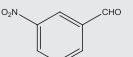
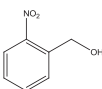
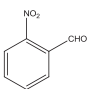
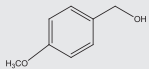
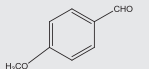
For optimizing the reaction conditions, we tried to convert benzyl alcohol (1 mmol) to benzaldehyde, as a model reaction, in the presence of the Fe<sub>3</sub>O<sub>4</sub>@HPEI/Pd catalyst

**TABLE 1** Oxidation of benzyl alcohol (1 mmol) in the presence of nanomagnetic catalyst

Entry	Catalyst (mol% of metal)	Oxidizing agent (mmol)	Solvent	Time (min)	Yield (%)
1	---	Oxone (1.2)	Water	65	20
2	Fe <sub>3</sub> O <sub>4</sub> @HPEI/Pd (1)	H <sub>2</sub> O <sub>2</sub> (1.2)	Cyclohexane	65	Trace
3	Fe <sub>3</sub> O <sub>4</sub> @HPEI/Pd (1)	H <sub>2</sub> O <sub>2</sub> (1.2)	Acetonitrile	65	20
4	Fe <sub>3</sub> O <sub>4</sub> @HPEI/Pd (1)	H <sub>2</sub> O <sub>2</sub> (1.2)	Ethanol	65	Trace
5	Fe <sub>3</sub> O <sub>4</sub> @HPEI/Pd (1)	H <sub>2</sub> O <sub>2</sub> (1.2)	Dichloromethane	65	15
6	Fe <sub>3</sub> O <sub>4</sub> @HPEI/Pd (1)	H <sub>2</sub> O <sub>2</sub> (1.2)	Dry toluene	65	Trace
7	Fe <sub>3</sub> O <sub>4</sub> @HPEI/Pd (1)	H <sub>2</sub> O <sub>2</sub> (1.2)	Solvent free	65	20
8	Fe <sub>3</sub> O <sub>4</sub> @HPEI/Pd (1)	H <sub>2</sub> O <sub>2</sub> (1.2)	Water	65	28
9	Fe <sub>3</sub> O <sub>4</sub> @HPEI/Pd (1)	O <sub>2</sub> atmosphere	Water	65	12
10	Fe <sub>3</sub> O <sub>4</sub> @HPEI/Pd (1)	Oxone (1.2)	Water	65	90
11	Fe <sub>3</sub> O <sub>4</sub> @HPEI/cu (1)	Oxone (1.2)	Water	65	55
12	Fe <sub>3</sub> O <sub>4</sub> @HPEI/co (1)	Oxone (1.2)	Water	65	48
13	Fe <sub>3</sub> O <sub>4</sub> @HPEI/Pd (1.5)	Oxone (1.2)	Water	65	90
14	Fe <sub>3</sub> O <sub>4</sub> @HPEI/Pd (0.5)	Oxone (1.2)	Water	65	64
15	Fe <sub>3</sub> O <sub>4</sub> @HPEI/Pd (0.25)	Oxone (1.2)	Water	65	30
16	Fe <sub>3</sub> O <sub>4</sub> @HPEI/Pd (1)	Oxone (0.8)	Water	65	89
17	Fe <sub>3</sub> O <sub>4</sub> @HPEI/Pd (1)	Oxone (0.6)	Water	65	90
18	Fe <sub>3</sub> O <sub>4</sub> @HPEI/Pd (1)	Oxone (0.5)	Water	65	80
19	Fe <sub>3</sub> O <sub>4</sub> @HPEI/Pd (1)	Oxone (0.3)	Water	65	55
20	Fe <sub>3</sub> O <sub>4</sub> @HPEI/Pd (1)	Absence (under N <sub>2</sub> atmosphere)	Water	120	0

<sup>a</sup> Yields refer to isolated products.

**TABLE 2** Oxidation of various alcohols using  $\text{Fe}_3\text{O}_4\text{@HPEI}$ Pd catalyst in water with oxone

$\begin{array}{c} \text{R}_1 \\   \\ \text{R}_2-\text{CH}-\text{OH} \end{array} \xrightarrow[\text{Water, rt}]{\text{Cat., Oxone}} \begin{array}{c} \text{R}_1 \\   \\ \text{R}_2-\text{C}=\text{O} \end{array}$ $\text{R}_1, \text{R}_2 = \text{Aryl, Alkyl, H}$				
Entry	Substrate	Product	Time (min)	Yield <sup>a</sup> (%)
1			65	90
2			70	89
3			65	93
4			70	90
5			80	91
6			65	89
7			65	90
8			70	91
9			70	88
10			70	87
11			120	86
12			120	85
13			120	85
14			45	94

(Continues)

TABLE 2 (Continued)

$\begin{array}{c} \text{R}_1 \\   \\ \text{R}_2-\text{CH}-\text{OH} \end{array} \xrightarrow[\text{Water, rt}]{\text{Cat., Oxone}} \begin{array}{c} \text{R}_1 \\   \\ \text{R}_2-\text{C}=\text{O} \end{array}$ <p><math>\text{R}_1, \text{R}_2 = \text{Aryl, Alkyl, H}</math></p>				
Entry	Substrate	Product	Time (min)	Yield <sup>a</sup> (%)
15			70	91
16			120	88
17 <sup>b</sup>			90	45
18		---	24 h	No product
19		---	24 h	No product
20 <sup>c,d</sup>			120	96.88
21 <sup>c</sup>			120	88.9
22 <sup>c</sup>			120	99.6

<sup>a</sup>Yields refer to isolated products. The products were characterized from their spectral data (IR, <sup>1</sup>H NMR) and compared with authentic samples.

<sup>b</sup>The reaction was followed by TLC (EtOAc-cyclohexane,3:10).

<sup>c</sup>The yields refer to GC analysis.

<sup>d</sup>The yield was 95.02% with 1 mol% of catalyst in 6 hrs at 80 °C and that was 99.30% with 1 mol% of catalyst in 24 hrs at r.t.

(30 mg, 1% mol of metal) and hydrogen peroxide (1.2 mmol was added in 3 steps) in various solvents (2 ml) at room temperature and the results are given in Table 1. The highest yield for benzaldehyde was achieved in water (entry 8). We investigated the effect of different oxidants on the oxidation of benzyl alcohol over Fe<sub>3</sub>O<sub>4</sub>@HPEI/Pd catalyst (1%mol) at room temperature. These results showed that the higher conversion was achieved with oxone as oxidant (entry 10). We also studied the oxidation of benzyl alcohol to benzaldehyde with other nanomagnetic catalysts (1% mol of metals,) and oxone. The results show that Fe<sub>3</sub>O<sub>4</sub>@HPEI/Pd is the best catalyst (entries 10–12). In addition, we observed that in the absence of catalyst the yield of oxidation with oxone is 20%.

The amount of the catalyst and oxidant were also optimized. The results showed that 30 mg of catalyst

(1 mol% of Pd) and 0.6 mmol (60 mol%) of oxidant is the best choice for the oxidation of 1 mmol of alcohol (entry 17). We also observed that benzyl alcohol was not oxidized with this system in the absence of oxidant under nitrogen atmosphere, even for long period of time (entry 20).

The competing reaction such as over oxidation of aldehydes to the corresponding carboxylic acids was not observed in any of the cases under above conditions, but the reaction produces by product corresponding carboxylic acid at high temperatures (>40 °C).

### 3.3 | Application scope

The optimized conditions were used for various alcohols to screen the generality of the work. As indicated in the Table 2, Fe<sub>3</sub>O<sub>4</sub>@HPEI/Pd catalyst showed higher efficiency than other nanomagnetic catalysts (Fe<sub>3</sub>O<sub>4</sub>@HPEI/



Co and  $\text{Fe}_3\text{O}_4@\text{PEI}/\text{Cu}$ ) for oxidation of a wide range of alcohols. This evidence could be resulted from relatively high redox potential of Pd in comparison with Co and Cu ( $E_{\text{Pd}^{2+}/\text{Pd}}^\circ = +0.951 \text{ V}$ ;  $E_{\text{Co}^{2+}/\text{Co}}^\circ = -0.280 \text{ V}$  and  $E_{\text{Cu}^{2+}/\text{Cu}}^\circ = +0.340 \text{ V}$ ). In most cases, the aldehyde selectivity was very high (>99%). The oxidation of various benzylic alcohols gave the carbonyl compounds in high yields and short reaction times. However, heterocyclic or heteroaromatic substrate containing oxygen or nitrogen atom seems to be poisonous for the catalyst.<sup>[45]</sup> For example, oxidation of piperonyl alcohol has low yield even in 24 hrs. (entry 17). In addition, 3-pyridinemethanol and 2-pyridinemethanol cannot produce corresponding aldehyde or carboxylic acid even for a long period of time (entries 18 and 19) and the catalyst inactivates a little at the end of the reaction. In comparison to benzylic alcohols, oxidation of aliphatic alcohols with this method did occur with longer reaction times.

To show the chemoselectivity of this method, the competitive reactions have been carried out in the presence of two alcohols (Supplementary data, Table S1, Figure S4 and Figure S5). The donor substituted group for example  $\text{CH}_3\text{O}^-$  group on the benzene ring of alcohol accelerates the reaction rate and the withdrawing groups (chloro- or carbonyl) reduced the reaction rate.

### 3.4 | Catalyst recycling

The catalyst was easily separated from the products by exposure of the reaction vessel to an external magnet and decantation of the reaction solution (Figure 3b). The remaining catalyst was washed repeatedly with acetone and water to remove undesired materials and dried to reuse. The catalyst showed excellent catalytic activity for more than 10 iterative cycles (Figure 6). The excellent activity and recyclability of catalyst in this reaction is

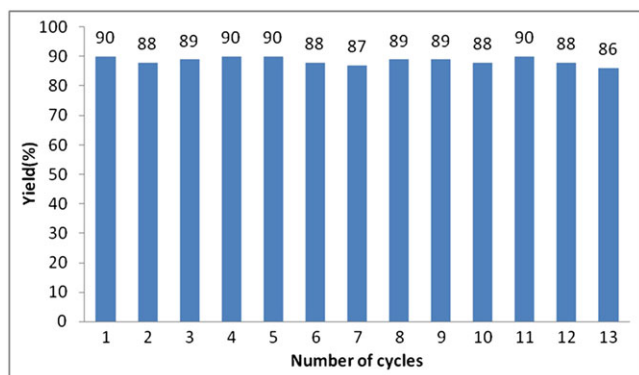
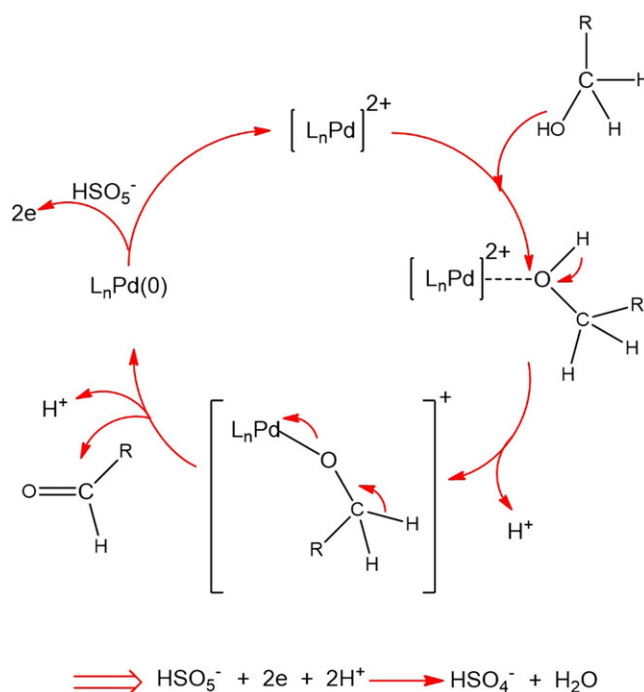


**FIGURE 6** Recyclability of the  $\text{Fe}_3\text{O}_4@\text{HPEI}/\text{Pd}$  catalyst for the oxidation of benzyl alcohol

illustrated by the finding that the 13th consecutive oxidation cycle was 86% complete after a reaction time of only 65 minutes. ICP analyzing showed that 3.36% of catalyst weight is palladium in 13th recycling. Therefore, it showed that no obvious diminishing palladium of the catalyst in 13th recycling. The TEM analysis suggests that the  $\text{Fe}_3\text{O}_4@\text{HPEI}/\text{Pd}$  nanoparticles in 13th recycling are almost spherical shapes and it shows that there is no obvious change of the catalyst in 13th recycling (Supplementary data, Figure S5).

### 3.5 | Proposed mechanism for the oxidation

Based on our experimental results and the related literature,<sup>[46,47]</sup> we propose the following reaction mechanism for the oxidation of alcohols by using oxone in the water and in the presence of  $\text{Fe}_3\text{O}_4@\text{HPEI}/\text{Pd}$  catalyst (Scheme 2). The common feature is that the formation of real oxidant is independent of catalyst Pd (II)-catalyzed oxidation of alcohols proceeds through a reduction of Pd (II) to Pd (0) by the alcohol. It seems that in  $\text{Fe}_3\text{O}_4@\text{HPEI}/\text{Pd}$ , PEI ligand as water soluble polymer which has several amine groups and facilitates oxidation of Pd(0) to Pd(II),<sup>[34]</sup> and then oxone ( $\text{HSO}_5^-$  in water) takes two electrons and the cycle continues in this mechanism.<sup>[48–50]</sup> Since the catalyst is present in the water phase,  $\text{HSO}_5^-$  takes electrons rapidly in contrast, when the palladium catalyst residues are in the organic phase,



**SCHEME 2** Proposed mechanism for the oxidation of alcohols with oxone in the presence of  $\text{Fe}_3\text{O}_4@\text{HPEI}/\text{Pd}$  catalyst

$\text{HSO}_5^-$  forms a separate aqueous phase, thus Pd(0) cannot donate electron.

## 4 | CONCLUSIONS

In conclusion, we have introduced a direct and effective method for the oxidation of alcohols to their corresponding carbonyl compounds utilizing oxone in the presence of  $\text{Fe}_3\text{O}_4@\text{HPEI}/\text{Pd}$  catalyst at room temperature in water. The use of non-toxic and inexpensive materials, stability of the oxidative system, simple method, short reaction times, good yields of the products and mild reaction conditions are the advantages of this method. In comparison with the other oxidants such as  $\text{O}_2$  or TBHP, oxidation with oxone accomplished at low temperatures and in short times.<sup>[51,52]</sup> The extension of the application of this nanocatalyst to different oxidation reactions is currently under investigation in our laboratory.

## ACKNOWLEDGEMENT

This work is funded by the grant NRF-2015-002423 of the National Research Foundation of Korea.

## REFERENCES

- [1] J. March, *Advanced Organic Chemistry: Reactions, Mechanisms, and Structure*, 4th ed., John Wiley and Sons, New York **1992**.
- [2] M. Hudlicky, *Oxidations in Organic Chemistry*, American Chemical Society, Washington DC **1990**.
- [3] R. C. Larock, *Comprehensive Organic Transformations: A Guide to Functional Group Preparations*, Wiley-VCH, New York **1999**.
- [4] G. Tojo, M. Fernandez, *Oxidation of Alcohols to Aldehydes and Ketones*, Berlin, Springer **2006**.
- [5] T. Lu, Z. Du, J. Liu, H. Ma, J. Xu, *Green Chem.* **2013**, *15*, 2215.
- [6] R. A. Sheldon, J. K. Kochi, *Metal-catalyzed Oxidation of Organic Compounds*, Academic Press, New York **1981**.
- [7] R. A. Sheldon, I. W. C. E. Arends, U. Isabel, *Green Chemistry and Catalysis*, Wiley-VCH, Weinheim, Germany **2007**.
- [8] E. Assady, B. Yadollahi, M. Riahi Farsani, M. Moghadam, *Appl. Organomet. Chem.* **2015**, *29*, 561.
- [9] Articles in PressX. Wang, S. Wu, Z. Li, X. Yang, J. Hu, Q. Huo, J. Guan, Q. Kan, *Appl. Organomet. Chem.* **2015**.
- [10] G. P. Anipsitakis, D. D. Dionysiou, *Environ. Sci. Technol.* **2003**, *37*, 4790.
- [11] Y. Cimen, H. Turk, *Appl. Catal. A: Gen.* **2008**, *340*, 52.
- [12] J. Madhavan, P. Maruthamuthu, S. Murugesan, S. Anandan, *Appl. Catal. B: Environ.* **2008**, *83*, 8.
- [13] L. A. Wozniak, W. J. Stec, *Tetrahedron Lett.* **1999**, *40*, 2637.
- [14] L. A. Wozniak, M. Koziolkiewicz, A. Kobylanska, W. J. Stec, *Bioorg. Med. Chem. Lett.* **1998**, *8*, 2641.
- [15] K. S. Webb, D. Levy, *Tetrahedron Lett.* **1995**, *36*, 5117.
- [16] K. S. Webb, S. J. Ruskay, *Tetrahedron* **1998**, *54*, 401.
- [17] B. M. Trost, D. P. Curran, *Tetrahedron Lett.* **1981**, *22*, 1287.
- [18] A. L. Baumstark, M. Beeson, P. C. Vasquez, *Tetrahedron Lett.* **1989**, *30*, 5567.
- [19] M. Bagherzadeh, M. Amini, D. M. Boghaei, M. M. Najafpour, V. McKee, *Appl. Organomet. Chem.* **2011**, *25*, 559.
- [20] P. Chutia, S. Kato, T. Kojima, S. Satokawa, *Polyhedron* **2009**, *28*, 370.
- [21] B. Liu, Y. Ren, Z. Zhang, *Green Chem.* **2015**, *17*, 1610.
- [22] Z. Zhang, J. Zhen, B. Liu, K. Lv, K. Deng, *Green Chem.* **2015**, *17*, 1308.
- [23] N. Mei, B. Liu, J. Zheng, K. Lv, D. Tang, Z. Zhang, *Catal. Sci. Technol.* **2015**, *5*, 3194.
- [24] B. Abbas Khakiani, K. Pourshamsian, H. Veisi, *Appl. Organomet. Chem.* **2015**, *29*, 259.
- [25] B. Liu, Z. Zhang, *ACS Catal.* **2016**, *6*, 326.
- [26] J. A. Melero, R. V. Grieken, G. Morales, *Chem. Rev.* **2006**, *106*, 3790.
- [27] D. Astruc, F. Lu, J. R. Aranzaes, *Angew. Chem. Int. Ed.* **2005**, *44*, 7852.
- [28] S. Morent, S. Vasseur, F. Grasset, E. Duguet, *J. Mater. Chem.* **2004**, *14*, 2161.
- [29] D. K. Yi, S. S. Lee, J. Y. Ying, *Chem. Mater.* **2006**, *18*, 2459.
- [30] H. Yoon, S. Ko, J. Jang, *Chem. Commun.* **2007**, 1468.
- [31] S. S. Banerjee, D. H. Chen, *Chem. Mater.* **2007**, *19*, 3667.
- [32] E. Ye, B. H. Liu, W. Y. Fan, *Chem. Mater.* **2007**, *19*, 3845.
- [33] B. J. Lopez, C. Boissiere, C. Chaneac, D. Grosso, S. Vasseur, S. Miraux, E. Duguet, C. Sanchez, *J. Mater. Chem.* **2007**, *17*, 1563.
- [34] A. Bhushan, H. Han, A. Sutherland, S. Boehme, F. Yaghmaie, C. E. Davis, *Appl. Organomet. Chem.* **2010**, *24*, 530.
- [35] P. R. Likhar, M. Roy, S. Roy, M. S. Subhas, M. L. Kantam, B. Sreedhara, *Adv. Synth. Catal.* **2008**, *350*, 1968.
- [36] B. Mu, P. Liu, Y. Dong, C. Lu, X. Wu, *J. Polym. Sci., Part A: Polym. Chem.* **2010**, *48*, 3135.
- [37] D. Zois, C. Vartzouma, Y. Deligiannakis, N. Hadjiliadis, L. Casella, E. Monzani, M. Loulodi, *J. Mol. Catal. A: Chem.* **2007**, *261*, 306.
- [38] J. Ho, F. M. Al-Deen, A. Al-Abboodi, C. Selomulya, S. D. Xiang, M. Plebanski, G. M. Forde, *Colloids Surf., B* **2011**, *83*, 83.
- [39] H. Zeng, Q. Lai, X. Liu, D. Wen, X. Ji, *J. Appl. Polym. Sci.* **2007**, *106*, 3474.
- [40] S. Li, W. Zhang, M. So, C. Che, R. Wang, R. Chen, *J. Mol. Catal. A: Chem.* **2012**, *359*, 81.
- [41] K. Esumi, R. Isono, T. Yoshimura, *Langmuir* **2004**, *20*, 237.
- [42] H. Ohde, C. M. Wai, H. Kim, J. Kim, M. Ohde, *J. Am. Chem. Soc.* **2002**, *124*, 4540.
- [43] L. P. Ramirez, K. Landfester, *Macromol. Chem. Phys.* **2003**, *204*, 22.

- [44] M. Khoobi, S. F. Motevalizadeh, Z. Asadgol, H. Forootanfar, A. Shafiee, M. A. Faramarzi, *Mater.Chem. Phys.* **2015**, *149*, 77.
- [45] Y. Kuang, Y. Nabae, T. Hayakawa, M. A. Kakimoto, *Appl. Catal. A: Gen.* **2012**, *423*, 52.
- [46] B. Karimi, A. Zamani, *J. Iran. Chem. Soc.* **2008**, *5*, 1.
- [47] J. Muzart, *Tetrahedron* **2007**, *63*, 7505.
- [48] K. S. Webb, S. J. Ruskay, *Tetrahedron* **1998**, *54*, 401.
- [49] Y. R. Wang, W. Chu, *Appl. Catal. B: Environ.* **2012**, *123*, 151.
- [50] S. P. Maradur, S. B. Halligudi, G. S. Gokavi, *Catal. Lett.* **2004**, *96*, 165.
- [51] M. B. Gawande, A. Rath, I. D. Nogueira, C. A. A. Ghumman, N. Bundaleski, O. M. N. D. Teodoro, P. S. Branco, *ChemPlusChem* **2012**, *77*, 865.
- [52] J. Tonga, L. Bo, Z. Li, Z. Lei, C. J. Xia, *Mol. Catal. A: Chem.* **2009**, *307*, 58.

## SUPPORTING INFORMATION

Additional Supporting Information may be found online in the supporting information tab for this article.

**How to cite this article:** Ramazani A, Khoobi M, Sadri F, et al. Efficient and selective oxidation of alcohols in water employing palladium supported nanomagnetic Fe<sub>3</sub>O<sub>4</sub>@hyperbranched polyethylenimine (Fe<sub>3</sub>O<sub>4</sub>@HPEI.Pd) as a new organic–inorganic hybrid nanocatalyst. *Appl Organometal Chem.* 2017;e3908. <https://doi.org/10.1002/aoc.3908>